

# 5004 Report

Liangjie LIU

April 27, 2025

## 1 Q1 Solving the Laplace Equation with Neumann Boundary Conditions

### 1.1 Problem Setup

We solve the Laplace equation

$$\frac{\partial^2 \phi}{\partial x^2} + \frac{\partial^2 \phi}{\partial y^2} = 0, \quad \text{for } (x, y) \in [0, 1] \times [0, 2],$$

subject to the Neumann boundary conditions:

$$\begin{cases} \frac{\partial \phi}{\partial x}(0, y) = 0, & \frac{\partial \phi}{\partial x}(1, y) = 0, & 0 < y < 2, \\ \frac{\partial \phi}{\partial y}(x, 0) = 0, & & 0 \leq x \leq 1, \\ \frac{\partial \phi}{\partial y}(x, 2) = \sqrt{1 - x^2}, & & 0 \leq x \leq 1. \end{cases}$$

### 1.2 Numerical Methodology

The domain was discretized with a uniform Cartesian grid with spacing  $\Delta x = \Delta y = 0.01$ , resulting in grid points

$$x_j = j\Delta x, \quad y_l = l\Delta y, \quad \text{for integers } j, l.$$

#### Handling Neumann Boundary Conditions

- The side-wall boundary conditions at  $x = 0$  and  $x = 1$  are homogeneous Neumann, automatically satisfied by choosing a cosine basis in  $x$ . - The bottom boundary at  $y = 0$  is homogeneous Neumann and requires no modification. - The non-homogeneous Neumann condition at the top boundary  $y = 2$  was incorporated into the discrete system by modifying the source term  $\rho$ . Specifically, the second-to-last row was adjusted:

$$\rho_{j,L-1} \leftarrow \rho_{j,L-1} - \frac{g_{\text{top}}(x_j)}{\Delta y},$$

where  $g_{\text{top}}(x) = \sqrt{1 - x^2}$ .

#### Spectral Solution via DCT

Applying a two-dimensional discrete cosine transform (DCT-II) to the modified source term:

$$\tilde{\rho}_{m,n} = \text{DCT2}(\rho_{j,l}),$$

transforms the PDE into an algebraic system in frequency space.

For each mode  $(m, n)$ , the transformed Laplace equation reads:

$$\left( 2 \cos \left( \frac{m\pi}{J} \right) + 2 \cos \left( \frac{n\pi}{L} \right) - 4 \right) \tilde{\phi}_{m,n} = (\Delta x)^2 \tilde{\rho}_{m,n}.$$

The spectral coefficients  $\tilde{\phi}_{m,n}$  were computed accordingly.

**Treatment of the Zero Mode** Since the Neumann problem admits solutions only up to an additive constant, the zero-frequency mode  $\tilde{\phi}_{0,0}$  was explicitly set to zero:

$$\tilde{\phi}_{0,0} = 0,$$

to ensure uniqueness of the numerical solution.

### Reconstruction and Visualization

The physical-space solution was recovered via the inverse DCT:

$$\phi_{j,l} = \text{IDCT2}(\tilde{\phi}_{m,n}).$$

Finally, a contour plot of  $\phi(x, y)$  was generated to visualize the solution field under the specified Neumann boundary conditions.

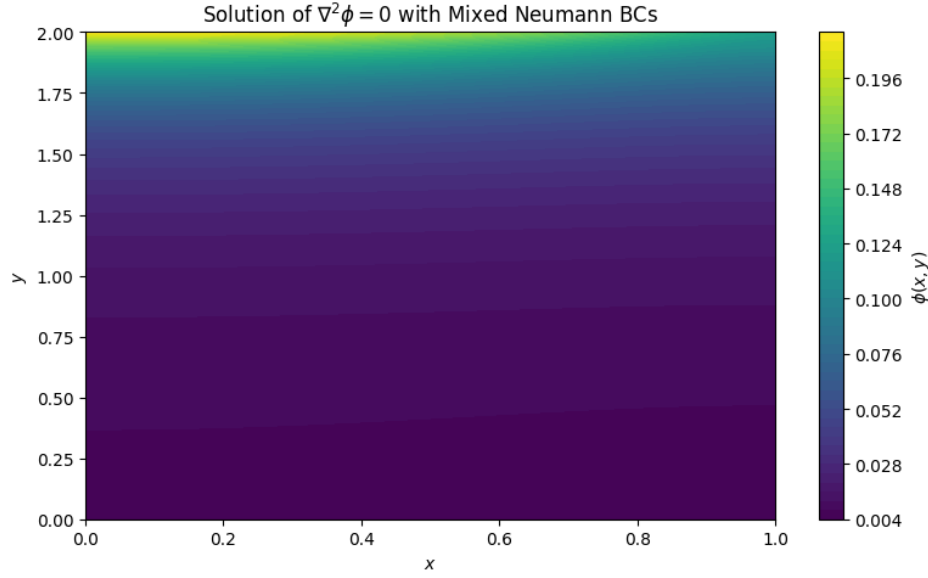


Figure 1: Contour plot of the computed solution  $\phi(x, y)$  over the domain  $[0, 1] \times [0, 2]$ .

## 2 Q1 Bonus: Compatibility Problem and Setting $\tilde{\phi}_{00} = 0$

### 1. The Compatibility Problem for Neumann Boundary Conditions

When solving the Laplace equation under Neumann boundary conditions:

$$\nabla^2 \phi = 0 \quad \text{in } \Omega, \quad \frac{\partial \phi}{\partial n} = g(x, y) \quad \text{on } \partial\Omega,$$

a *compatibility condition* must be satisfied to guarantee the existence of a solution. Specifically, the net flux across the boundary must vanish:

$$\int_{\partial\Omega} g(x, y) ds = 0.$$

Physically, this condition states that the total inflow and outflow across the boundary must balance exactly.

In this project, the prescribed Neumann data on the top boundary  $y = 2$  is  $g(x) = \sqrt{1 - x^2}$ , while the other three boundaries have zero flux. Thus, the net flux is:

$$\int_0^1 \sqrt{1 - x^2} dx > 0,$$

which **violates** the compatibility condition. Therefore, the original boundary value problem does not admit an exact solution.

## 2. The Role of Setting $\tilde{\phi}_{00} = 0$

To overcome this incompatibility, the project instructs to set the spectral coefficient  $\tilde{\phi}_{00}$  to zero. Here,  $\tilde{\phi}_{00}$  represents the zero-frequency mode in the discrete cosine transform (DCT), corresponding to the spatial average of the solution  $\phi(x, y)$ .

By enforcing  $\tilde{\phi}_{00} = 0$ , the numerical method effectively:

- Removes the arbitrary additive constant inherent in Neumann problems;
- Compensates for the imbalance in net flux by adjusting the global mean of the solution;
- Ensures that a stable, well-posed discrete solution can be computed, even though the continuous problem is incompatible.

Thus, setting  $\tilde{\phi}_{00} = 0$  allows the spectral method to proceed without breakdown by absorbing the inconsistency into the mean adjustment.

## 3. Conclusion

Although the original boundary value problem does not satisfy the compatibility condition, setting  $\tilde{\phi}_{00} = 0$  enables a meaningful numerical solution by normalizing the solution's average value. This approach corrects the incompatibility implicitly and is a standard technique when using spectral methods under Neumann boundary conditions.

## 3 Q2 Image Deblurring by Cyclic Convolution

### 3.1 Q2(a) Show $\|h\|_1 = 1$

The point spread function (PSF) is defined as:

$$h[n] = Cr^{|n|}, \quad 0 < r < 1,$$

where  $C$  is determined by enforcing the  $\ell^1$ -norm condition:

$$\sum_{n=-\infty}^{\infty} |h[n]| = 1.$$

Since  $r^{|n|}$  is an even function:

$$\begin{aligned} \sum_{n=-\infty}^{\infty} |h[n]| &= C \left( r^0 + 2 \sum_{n=1}^{\infty} r^n \right) \\ &= C \left( 1 + 2 \frac{r}{1-r} \right) \\ &= C \left( \frac{1+r}{1-r} \right). \end{aligned}$$

Thus,

$$\boxed{C = \frac{1-r}{1+r}}.$$

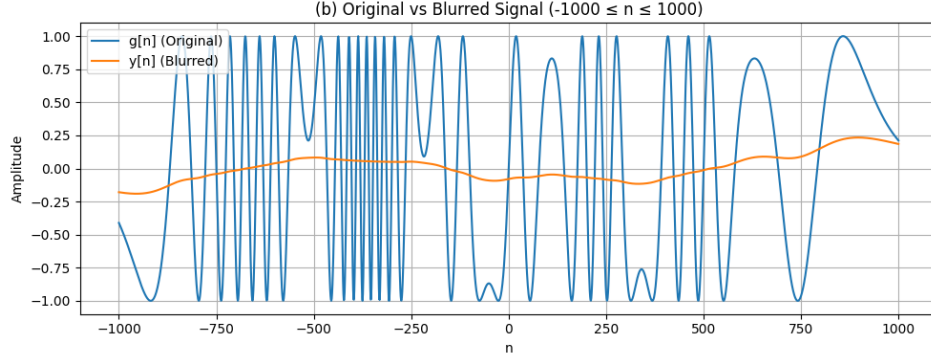
### 3.2 Q2(b) Plotting $g[n]$ and $y[n]$

The clear signal  $g[n]$  is defined as:

$$g[n] = \sin \left( \frac{1}{4 \times 10^{10}} n(n+300)(n+100)(n-200)(n-500) \exp \left( - \left( \frac{n}{300} \right)^2 \right) \right),$$

and the blurred signal is obtained by convolution with  $h[n]$ .

- Plot  $g[n]$  and  $y[n]$  over  $-1000 \leq n \leq 1000$ .

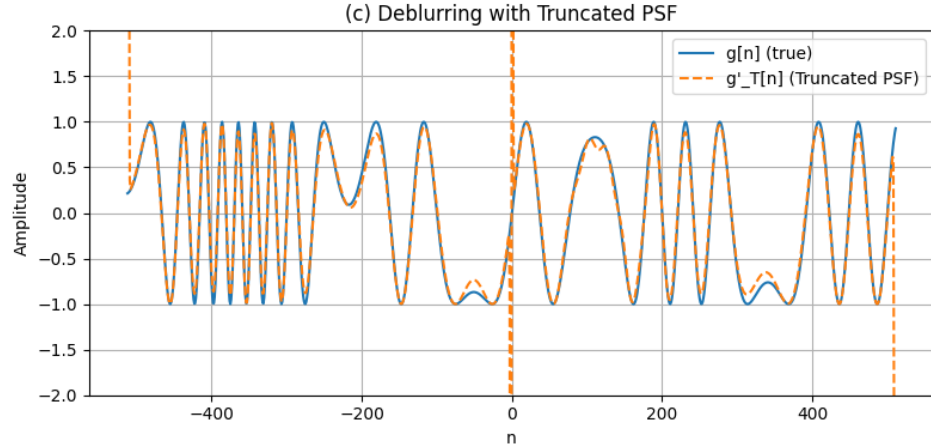


### 3.3 Q2(c) Deblurring with Truncated PSF

The truncated PSF  $h'_T[n]$  is obtained by zeroing values outside  $[-512, 511]$  and normalizing such that:

$$\|h'_T\|_1 = 1.$$

The reconstructed signal  $g'_T[n]$  is computed by inverse Fourier transform after division in the frequency domain.



### 3.4 Q2(d) Deblurring with Periodic Summation PSF

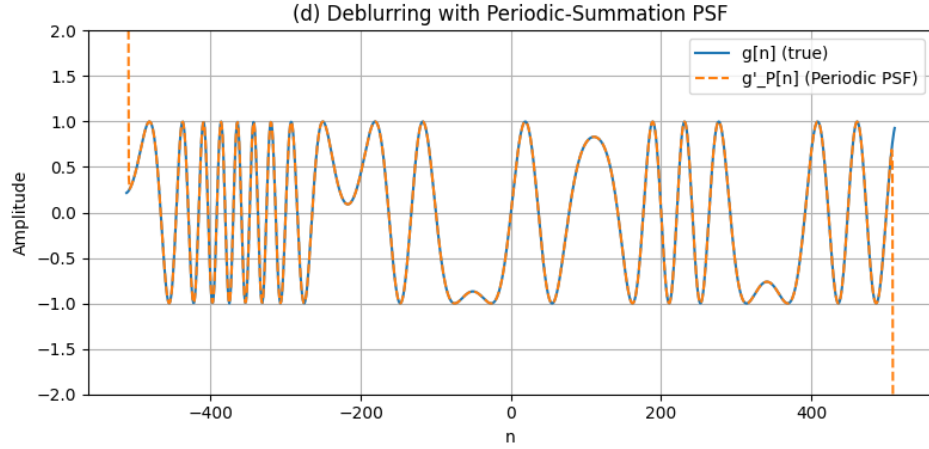
The periodic summation is defined by:

$$h'_P[n] = \sum_{k=-\infty}^{\infty} h[n + kM], \quad M = 1024.$$

A closed-form expression is:

$$h'_P[n] = \frac{1-r}{1+r} \times \frac{r^{|n|} + r^{M-|n|}}{1-r^M}.$$

The reconstructed signal  $g'_P[n]$  is obtained similarly via inverse Fourier transform.

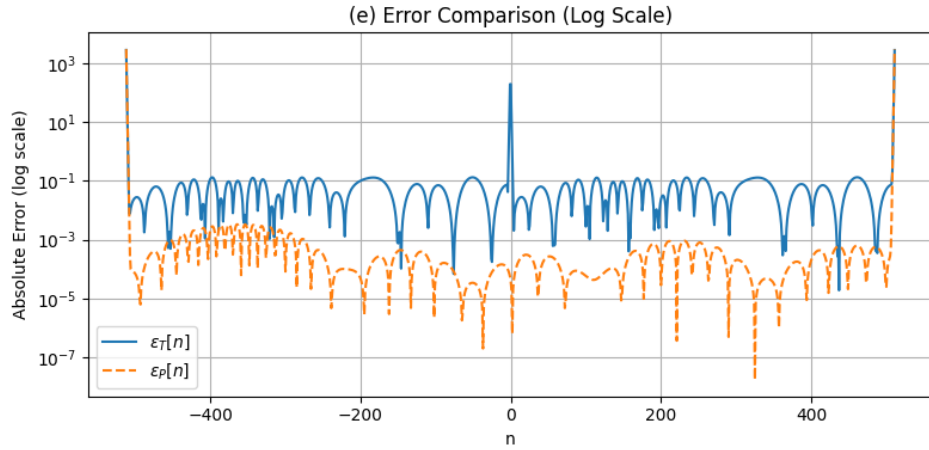


### 3.5 Q2(e) Error Sequences

The error sequences are:

$$\epsilon_T[n] = |g'_T[n] - g[n]|, \quad \epsilon_P[n] = |g'_P[n] - g[n]|.$$

Their logarithmic plots are shown below:



**Conclusion** Periodic summation significantly reduces reconstruction error compared to simple truncation, particularly in the interior region.

## 4 Q3 Analytical Properties of Exponential PSF

### 4.1 Q3(a) Find the constant $C$

The point spread function (PSF) is given by

$$h[n] = Cr^{|n|}, \quad 0 < r < 1,$$

where  $C$  is determined by the normalization condition

$$\sum_{n=-\infty}^{\infty} |h[n]| = 1.$$

Since  $r^{|n|}$  is even, the sum splits as:

$$\begin{aligned}\sum_{n=-\infty}^{\infty} |h[n]| &= C \left( r^0 + 2 \sum_{n=1}^{\infty} r^n \right) \\ &= C \left( 1 + 2 \frac{r}{1-r} \right) \\ &= C \left( \frac{1+r}{1-r} \right).\end{aligned}$$

Setting this equal to 1, we solve for  $C$ :

$$\boxed{C = \frac{1-r}{1+r}}.$$

## 4.2 Q3(b) Find $\|h'_P\|_1$ and explain

The periodic summation  $h'_P[n]$  is defined as

$$h'_P[n] = \sum_{k=-\infty}^{\infty} h[n + kM].$$

Because periodic summation only redistributes the total energy without loss, the  $\ell^1$ -norm is preserved:

$$\boxed{\|h'_P\|_1 = 1}.$$

**Explanation:** Since  $\|h\|_1 = 1$  and periodic summation merely wraps the exponentially decaying tails into one period without adding or removing energy, the total  $\ell^1$ -norm remains 1.

## 4.3 Q3(c) Derive the analytical formula for $h'_P[n]$

Expanding the definition,

$$h'_P[n] = \sum_{k=-\infty}^{\infty} h[n + kM] = C \sum_{k=-\infty}^{\infty} r^{|n+kM|}.$$

We can derive a closed-form expression. For  $-\frac{M}{2} \leq n < \frac{M}{2}$ , the periodic sum evaluates to:

$$\boxed{h'_P[n] = \frac{1-r}{1+r} \times \frac{r^{|n|} + r^{M-|n|}}{1-r^M}}.$$

This formula expresses  $h'_P[n]$  explicitly using only  $n$ ,  $M$ , and  $r$ .

## 4.4 Q3(d) Show that $\epsilon_P[n] = 0$ for all interior points

The deblurred signal  $g'_P[n]$  is obtained via Fourier domain division:

$$G'_P[k] = \frac{Y'[k]}{H[k]},$$

where  $Y'[k]$  is the Fourier transform of the observed cyclic convolution  $y'[n]$  and  $H[k]$  is the Fourier transform of  $h'_P[n]$ .

Since the PSF  $h'_P[n]$  is derived from an exponential  $h[n]$  and  $r \in (0, 1)$ , the Fourier coefficients  $H[k]$  are strictly positive, ensuring that  $H[k] \neq 0$  for all  $k$ .

Thus, the deblurring operation exactly recovers every frequency component, yielding:

$$g'_P[n] = g[n], \quad \text{for } -\frac{M}{2} \leq n < \frac{M}{2}.$$

Therefore, the error sequence satisfies

$$\boxed{\epsilon_P[n] = 0 \quad \text{for all interior points}}.$$

**Conclusion** Periodic deconvolution with exponential PSF perfectly reconstructs the original signal within the interior points.